Cell Reports, Volume *35*

Supplemental information

Microglia provide structural resolution to injured dendrites after severe seizures

Ukpong B. Eyo, Koichiro Haruwaka, Mingshu Mo, Antony Brayan Campos-Salazar, Lingxiao Wang, Xenophon S. Speros IV, Sruchika Sabu, Pingyi Xu, and Long-Jun Wu

Supplemental Information

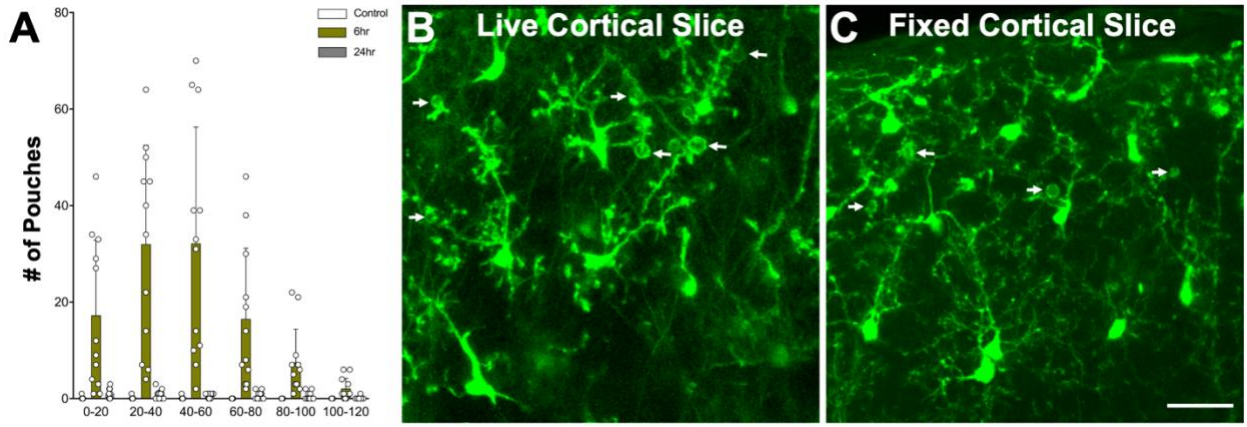

Figure S1. Microglial process pouches occur independent of craniotomy surgeries. Related to Figure 1.

(**A**) Quantification of microglial process pouch numbers in specific fields of view at varying depths with sham control as well as 6h and 24hr of KA-induced seizures at 6h.

(**B**) Representative two-photon image of a live cortical brain slice freshly generated from a CX3CR1$^{GFP/+}$ mouse at 6h of KA treatment showing microglial process pouch in superficial cortical regions (white arrows).

(**C**) Representative two-photon image of a fixed cortical brain slice from a CX3CR1$^{GFP/+}$ mouse at 6h of KA treatment showing microglial process pouch in superficial cortical regions (white arrows). Scale bar: 20µm

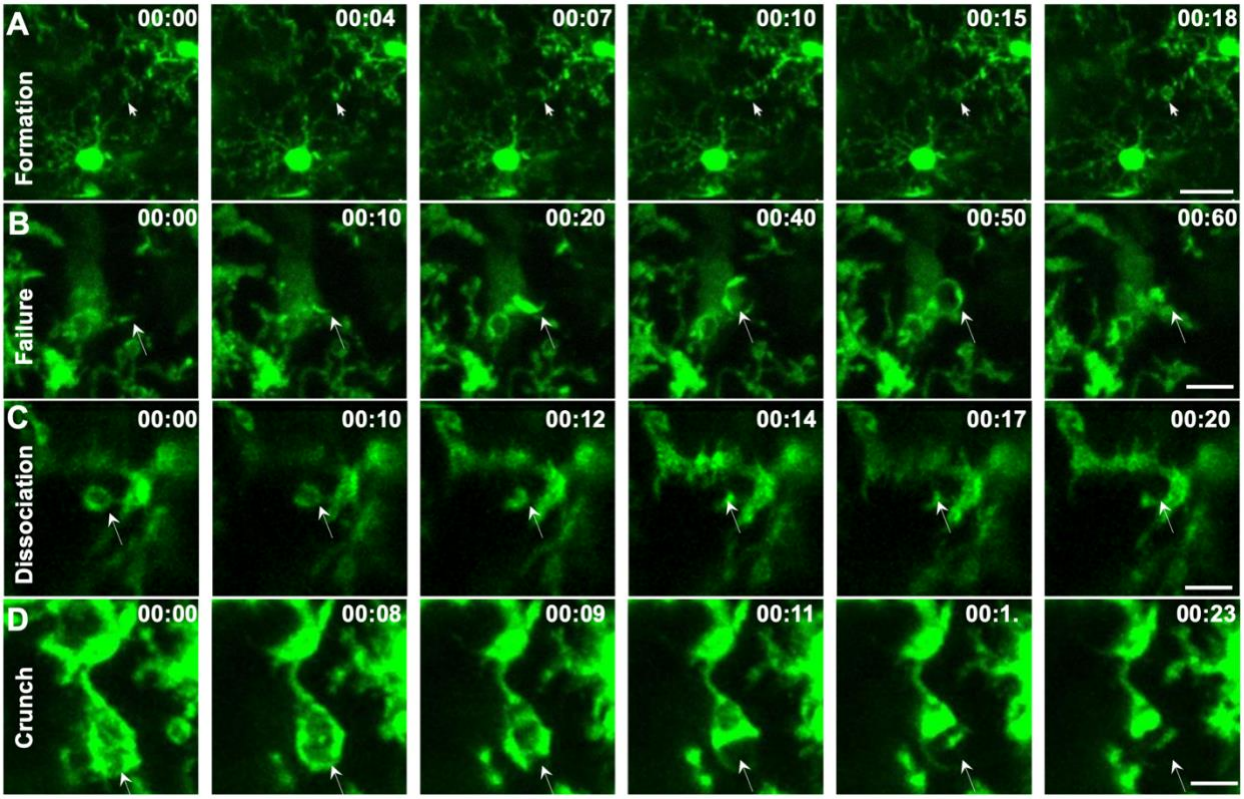

Figure S2. Formation and resolution of microglial process pouches. Related to Figure 2.
(**A**) Representative two-photon *in vivo* images from a time-lapse movie generated from a CX3CR1$^{GFP/+}$ mouse showing the temporal formation of a microglial process pouch after frisking activity (white arrow). Scale bar: 20µm.
(**B**) Representative two-photon *in vivo* images from a time-lapse movie generated from a CX3CR1$^{GFP/+}$ mouse showing the failure to form a microglial process pouch during frisking activity (white arrow). Scale bar: 20µm.
(**C**) Representative two-photon *in vivo* images from a time-lapse movie generated from a CX3CR1$^{GFP/+}$ mouse showing dissociation of a microglial process pouch by gradual withdrawal (white arrow). Scale bar: 20µm.
(**D**) Representative two-photon *in vivo* images from a time-lapse movie generated from a CX3CR1$^{GFP/+}$ mouse showing rapid collapse of a microglial process pouch by a rapid “crunch” (white arrow). Scale bar: 5µm.

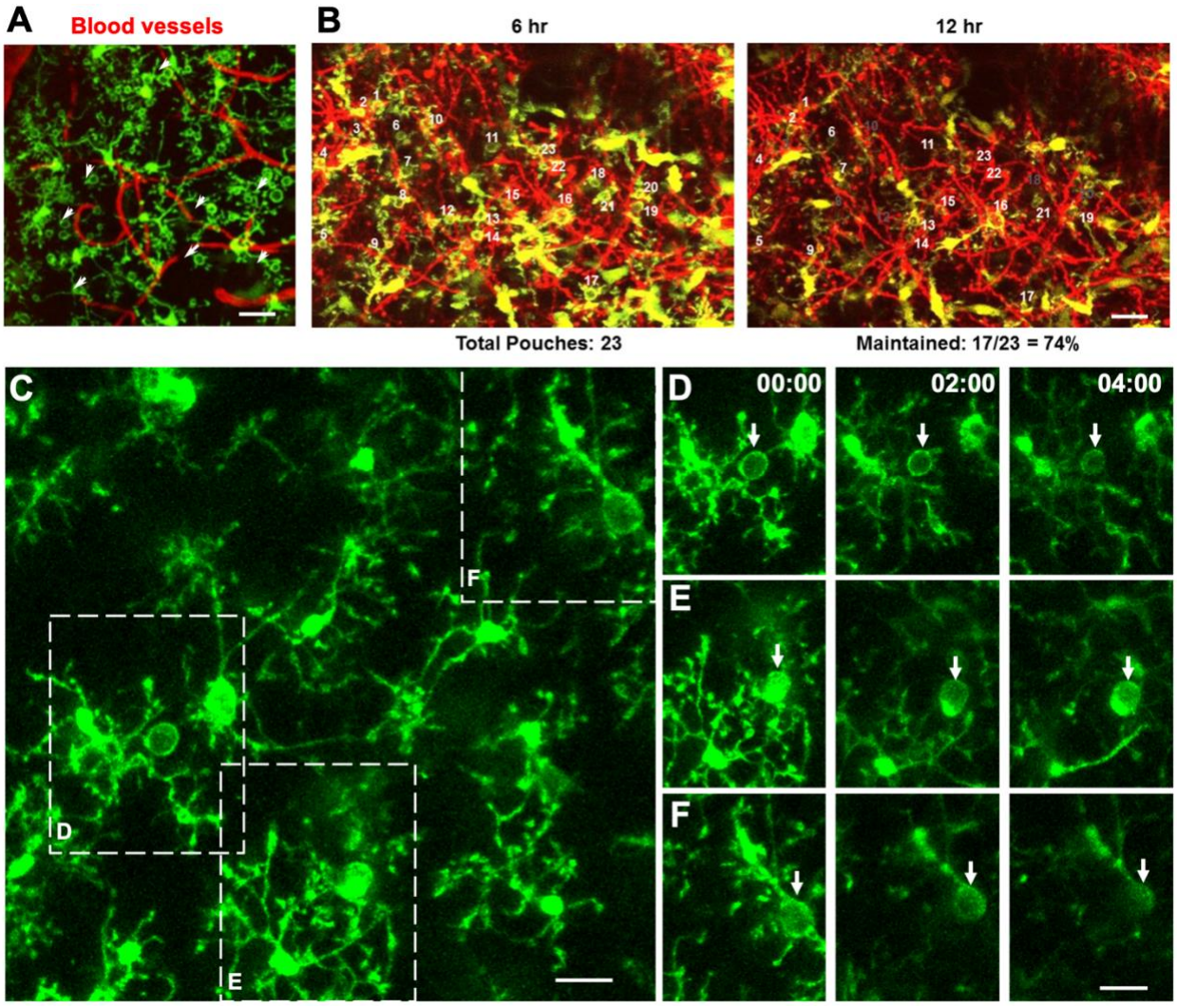

Figure S3. Microglial process pouches remain stable independent of anesthesia or craniotomy surgery. Related to Figure 2.

(**A**) Representative two-photon *in vivo* image from a CX3CR1$^{GFP/+}$ mouse showing microglial pouches and the vasculature (2mg/mL i.p. Rhodamine B) at 6h of KA treatment. Scale bar: 20µm.

(**B**) Representative two-photon *in vivo* images from a CX3CR1$^{GFP/+}$:Thy1^{YFP} mouse showing microglial pouches identified with numbers at 6h and then re-imaged at 24h after KA. Scale bar: 20µm.

(**C**) Representative two-photon *in vivo* image from a CX3CR1$^{GFP/+}$ mouse brain slice freshly prepared at 6h of KA. Scale bar: 10µm.

(**D**-**F**) Representative time-lapse images from various fields of view in (**C**) showing pouches that are maintained from throughout the imaging period (white arrows). Scale bar: 5µm.

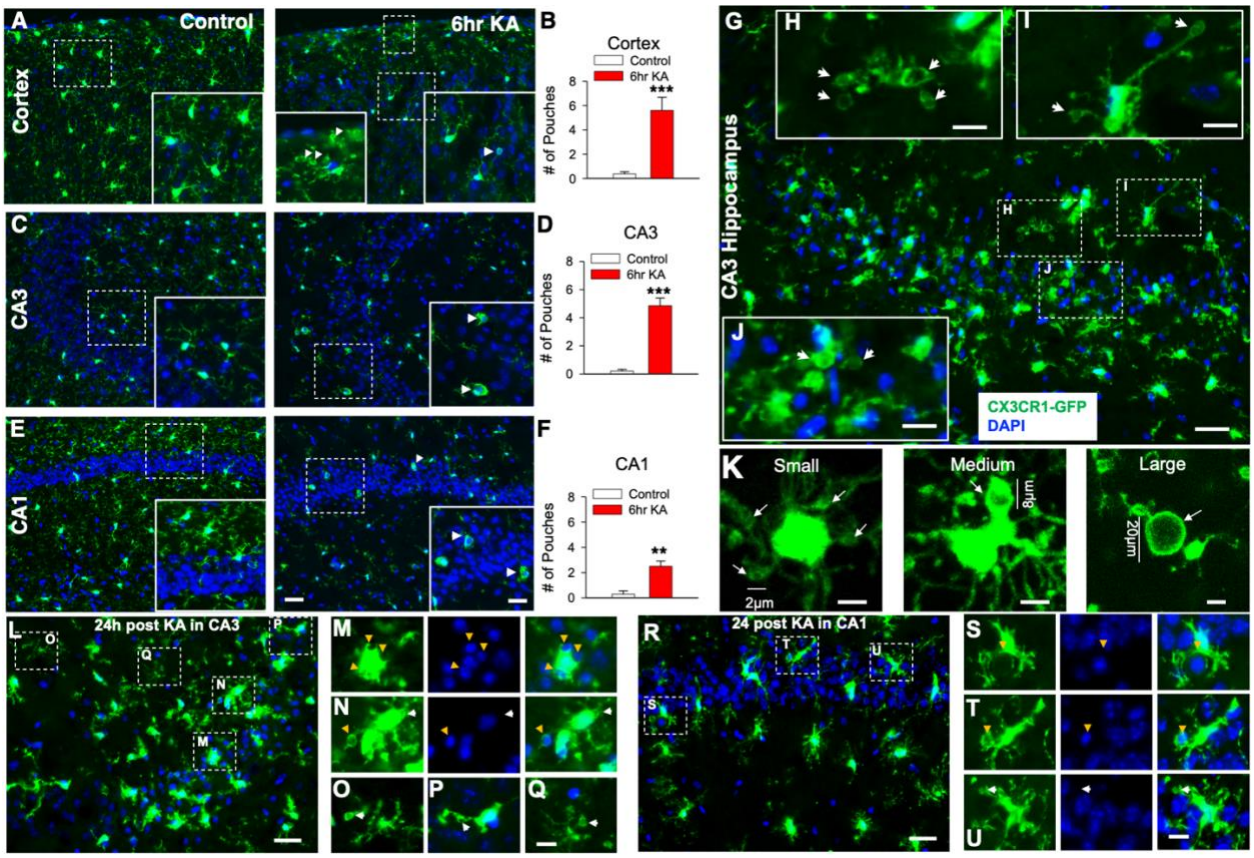

Figure S4. Seizure-induced microglial process pouches often target non-nucleic material. Related to Figure 4.

(**A**) Representative images from fixed CX3CR1$^{GFP/+}$ control and seizure mouse brain slices at 6h showing pouch numbers in the cortex.

(**B**) Quantification of the cortical pouches from fixed control and seizure mouse brain slices at 6h (n = 3 mice each).

(**C**) Representative images from fixed CX3CR1$^{GFP/+}$ control and seizure mouse brain slices at 6h showing pouch numbers in the CA3 region of the hippocampus.

(**D**) Quantification of the CA3 pouches from control and seizure slices at 6h (n = 3 mice each).

(**E**) Representative images from fixed CX3CR1$^{GFP/+}$ control and seizure mouse brain slices at 6h showing pouch numbers in the CA1 region of the hippocampus. Scale bar: 25µm and 10µm for the insert.

(**F**) Quantification of the CA1 pouches from control and seizure slices at 6h (n = 3 mice each).

(**G-J**) Representative images from a fixed CX3CR1$^{GFP/+}$ mouse brain slice at 6h showing several pouches (inserts) lacking DAPI. Scale bar: 25µm and 5µm for inseerts

(**K**) Representative two-photon *in vivo* images of pouches of different sizes. Scale bar: 5µm.

(**L**) Representative image from fixed CX3CR1$^{GFP/+}$ mouse brain slices showing pouches in the CA3 region of the hippocampus. Scale bar: 25µm.

(**M**-**Q**) Representative enlarged images of boxed regions in (**L**) showing microglial pouches with around DAPI-labelled nuclei (yellow arrows) and pouches without DAPI (white arrows). Scale bar: 5µm.

(**R**) Representative image from fixed CX3CR1$^{GFP/+}$ mouse brain slices showing pouches in the CA1 region of the hippocampus. Scale bar: 25µm.
(**S**-**U**) Representative enlarged images of boxed regions in (K) showing microglial pouches with around DAPI-labelled nuclei (yellow arrows) and pouches without DAPI (white arrows). Data is presented as mean ± SEM. Scale bar: 5µm.

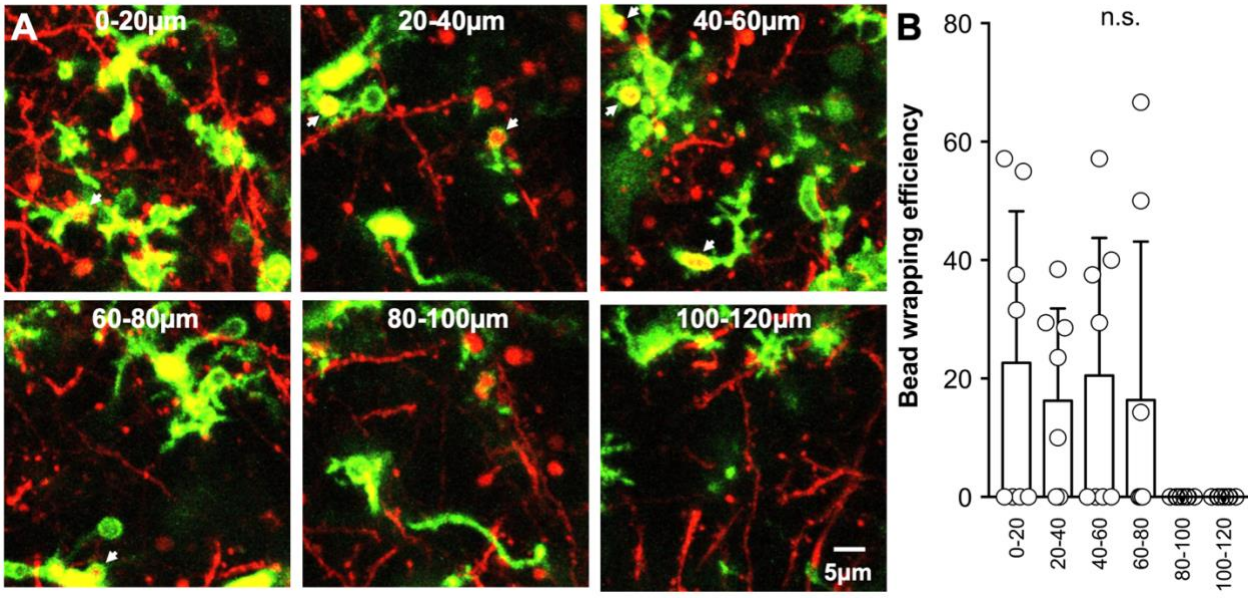

Figure S5. Microglial pouch-bead interactions at 6hr. Related to Figure 4.
(**A**) Representative images from *in vivo* imaging in double transgenic CX3CR1$^{GFP/+}$: Thy1^{YFP} mice following seizures. z-projection images of varying depth showing pouch wrapping of dendritic beads (arrows). Scale bar: 5µm.
(**B**) Quantification of the microglial pouch-bead wrapping at various depths at 6h of seizures (n = 10 mice). Data is presented as mean ± SEM.